ISPRS Journal of Photogrammetry and Remote Sensing 220 (2025) 264–276

Contents lists available at ScienceDirect

ISPRS Journal of Photogrammetry and Remote Sensing

journal homepage: www.elsevier.com/locate/isprsjprs

Detection of non-stand replacing disturbances (NSR) using Harmonized Landsat-Sentinel-2 time series

Madison S. Brown [a,*], Nicholas C. Coops [a], Christopher Mulverhill [a], Alexis Achim [b]

[a] Integrated Remote Sensing Studio, Department of Forest Resource Management, University of British Columbia, 2424 Main Mall, Vancouver, BC V6T 1Z4, Canada
[b] Centre de recherche sur les matériaux renouvelables, Département des sciences du bois et de la forêt, Université Laval, Québec, QC G1V 0A6, Canada

ARTICLE INFO

Keywords:
Continuous Forest Inventory
Forest monitoring
Change detection
Insects
HLS
Landsat

ABSTRACT

Non-stand replacing disturbances (NSRs) are events that do not result in complete removal of trees and generally occur at a low intensity over an extended period of time (e.g., insect infestation), or at spatially variable intensities over short time intervals (e.g., windthrow). These disturbances alter the quality and quantity of forest biomass, impacting timber supply and ecosystem services, making them critical to monitor over space and time. The increased accessibility of high frequency revisit, moderate spatial resolution satellite imagery, has led to a subsequent increase in algorithms designed to detect sub-annual change in forested landscapes across broad spatial scales. One such algorithm, the Bayesian Estimator of Abrupt change, Seasonal change, and Trend (BEAST) has shown promise with sub-annual change detection in temperate forested environments. Here, we evaluate the sensitivity of BEAST to detect NSRs across a range of severity levels and disturbance agents in Central British Columbia (BC), Canada. Moderate resolution satellite time series data were utilized by BEAST to produce rasters of change probability, which were compared to the occurrence, severity, and timing of disturbances as mapped by the annual British Columbia Aerial Overview Survey (BC AOS). Differences in the distributions of BEAST probabilities between agents and levels of severity were then compared to undisturbed pixels. In order to determine the applicability of the algorithm for updating forest inventories, BEAST probability distributions of major NSRs (> 5 % of total AOS disturbed area) were compared between consecutive years of disturbances. Cumulatively, all levels of disturbances had higher and statistically significant ($p < 0.05$) mean BEAST change probabilities compared with historically undisturbed areas. Additionally, 16 disturbance agents observed in the area had higher statistically significant ($p < 0.05$) probabilities. All major NSRs showed an upwards and statistically significant ($p < 0.05$) progression of BEAST probabilities over time corresponding to increases in BC AOS mapped area. The sensitivity of BEAST change probabilities to a wide range of NSR disturbance agents at varying intensities suggests promising opportunities for earlier detection of NSRs to inform continuously updating forest inventories and potentially inform adaptation and mitigation actions.

1. Introduction

Disturbances impact forest distribution, abundance, composition, and structure (Cohen et al., 2016) and there is mounting evidence to suggest terrestrial disturbances attributed to climate change and other forms of anthropogenic landscape modification are increasing globally (Shi et al., 2021; Van Mantgem et al., 2009). With such intensification of disturbance regimes, site features previously considered intrinsic to a forest (i.e., microclimate, soil chemistry) are being altered and in turn act as drivers of a shift in forest attributes (e.g., height, canopy cover, above-ground biomass, etc.) and ecology (Achim et al., 2022; Agee, 1993).

The impact of disturbances on both the individual tree and stand level is heavily agent dependent. Stand-replacing disturbances (SRs) are events that result in the complete removal of trees (Swanson et al., 2011; Bender et al., 1984). With the newly available growing space, pioneer species often regenerate rapidly to form even-aged cohorts that dominate post-disturbance landscapes. In contrast, non-stand replacing disturbances (NSRs) do not result in complete removal of trees and generally occur at a lower intensity over a longer period of time (e.g., insect infestation, drought), or at spatially variable intensities over a shorter interval (e.g., windthrow, low-moderate intensity fire, frost;

* Corresponding author at: 2424 Main Mall, Vancouver, BC V6T 1Z4, Canada.
E-mail address: madib98@student.ubc.ca (M.S. Brown).

https://doi.org/10.1016/j.isprsjprs.2024.12.014
Received 1 August 2024; Received in revised form 24 October 2024; Accepted 13 December 2024
Available online 20 December 2024

Oliver & Larson, 1996; Payette et al., 1990; Bigler et al., 2005; Hermosilla et al., 2019). These variable disturbance intensities and spatial patterns often lead to more heterogenous stand structures in terms of distribution and quantity of biomass (Peng et al., 2011).

The overall structural change in forest stands associated with NSRs impact both timber supply and ecosystem services, in addition to acting as a key driver of forest composition shifts and changes in biomass dynamics (Morin-Bernard et al., 2023; Woods, 2000; Woods & Kern, 2022). For example, insect outbreaks throughout North America are increasing the mortality of overstory trees resulting in more growth of secondary structure (e.g., seedlings, saplings, sub-canopy trees, shrubs, herbs, and surviving canopy trees; Ye et al., 2021). This can, in turn, lead to an increase in decomposing biomass, and carbon released due to this decomposition and impacts habitat, soil quality, nutrient cycling, etc. (Brown et al., 2010; Carroll et al., 2004). Low- to moderate-intensity fire can also alter forest structure; tree falling paired with loss of foliage on some charred trees can increase light and resource availability; altering species diversity, soil carbon availability and water holding capacity. This can result in an ecological and structural shift post-fire (Meigs et al., 2020; Parks et al., 2018; Zald & Dunn, 2018).

In Canada, forest inventories are designed to determine the location, extent, condition, composition, and structure of forests, and play a key role in the sustainable management of resources (Kangas & Maltamo, 2006; Tompalski et al., 2021; White et al., 2016). Conventional strategic forest inventories generally occur each decade and involve the acquisition of aerial images that are interpreted to generate a polygonal layer representing forest stands within which attributes are estimated. Attributes of interest such as height, species, volume, diameter at breast height (DBH), and stem density are taken from ground-based measurements and then linked to the interpreted polygons forming the baseline of inventories (Gillis & Leckie, 1996; Thompson et al., 2007). As 10-year surveys are generally not adequate for consistent monitoring of disturbance, mapping of NSRs is often supplemented as part of annual provincial or national forest health surveys which are undertaken from the air, and augmented by field plots (Westfall & Ebata, 2019).

These forest health surveys, (e.g., British Columbia Aerial Overview Survey (BC AOS)) are generally updated annually and produce broad-scale polygon layers with attributed severity and disturbance agents (Westfall & Ebata, 2019; Gillis & Leckie, 1996). This monitoring method broadly provides robust information for long-term monitoring but are often limited when identifying precise spatial locations of outbreaks and observing the progression of changes within the year. Additionally, aerial overview surveys are dependent on expert personnel and equipment to map and observe disturbance patterns, which can incur high costs (Westfall & Ebata, 2019) and demonstrates a need for alternate data sources and continuous inventory methods (Achim et al., 2022; Coops et al., 2020; Culvenor et al., 2014; Giannetti et al., 2021; Hyyppä et al., 2020).

Satellite-based remote sensing methods can help address these challenges. Previous studies have shown that satellite imagery can be effectively used to detect and map forest disturbances (Hansen & Loveland, 2012); however, the reliability of detection is highly dependent on their severity and extent (Stone et al., 2001). NSRs such as Mountain Pine Beetle (MPB; *Dendroctonus ponderosae*), Spruce Beetle (*Ips typographus*), and Spruce Budworm (*Choristoneura fumiferana*) have been detected using satellite time series (Coops et al., 2006; DeRose et al., 2011; Franklin et al., 2008; Goodwin et al., 2010; Hilker et al., 2009; Meddens et al., 2013) but studies have often performed detection retrospectively (i.e. after the disturbance has reached a epidemic level). Challenges exist with these methods when detecting lower intensity NSRs, thereby driving the need for methods that capture more incremental deviation (Coops et al., 2006; Jarron et al., 2017).

The increase of the temporal frequency of satellite imagery has enabled further development of methods to detect linear, or more complex (e.g., sinusoidal) changes in the spectral response of vegetation (Coops et al., 2008). This is done using a variety of different algorithms such as LandTrendr (Kennedy et al., 2010; Senf et al., 2015), CCDC (Zhu &Woodcock, 2014), BFAST (Verbesselt et al., 2010), and Composite2Change (Hermosilla et al., 2016). These methods have been applied using annual image composites and continuously, using time series of images (Coops et al., 2020; Hermosilla et al., 2016; Kennedy et al., 2010).

Annual composites allowing pixels to be compared at similar times of the year reducing the effect of phenological variation (Coops et al., 2020). Annual timesteps are successful for long-term monitoring; however, they may not meet data requirements for forest managers aiming to implement sub-annual operational changes (Bontemps et al., 2022; Coops et al., 2023; Melaas et al., 2013; Mulverhill et al., 2023). Continuous change detection has been most often tested in areas with little seasonal spectral variation such as tropical forests (Chen et al., 2021; Reiche et al., 2018; Shang et al., 2022). However, such approaches have not been as widely applied in regions with high seasonal variation such as those of temperate forests in North America (Mulverhill et al., 2023; Seyednasrollah et al., 2021).

Mulverhill et al. (2023) examined specifically the issue of seasonality impacting continuous change detection utilizing the Bayesian Estimator of Abrupt Change, Seasonality, and Trend (BEAST) algorithm. BEAST has shown promise in filling gaps of optical time series of satellite data making it a good choice for continuous change detection in areas of high seasonal variation (Hu et al., 2021; Zhao et al., 2019). To examine if the algorithm could be used in a continuous monitoring scenario, image composites from a dense times series of Landsat and Harmonized Landsat Sentinel-2 were successively added, and the algorithm was re-run with the addition of a new image. When compared with a validation dataset in dry interior coniferous forest ecosystems, Mulverhill et al. (2023) found that the BEAST algorithm had a 43.7 % within ≈ 144 days, 66.8 % within ≈ 192 days, and 89.9 % detection rate for all disturbances within ≈ 288 days. These results demonstrate the algorithm's success at capturing disturbance at sub-annual scales, presenting an opportunity for its application for continuous change detection (Giannetti et al., 2021; Hu et al., 2021; Mulverhill et al., 2023).

However, as effective monitoring of NSRs is critical to any forest inventory, the overall objective of this study is to specifically assess the BEAST algorithm's ability to detect NSRs in the context of a continuous forest inventory (Coops et al., 2023). This is broken down into the following three sub-objectives: (1) assess BEAST's sensitivity to NSRs at varying levels of severity, (2) assess BEAST's sensitivity to NSRs of varying disturbance agents, and (3) examine the applicability of BEAST to be integrated into continuous forest inventories. To do so, we applied the BEAST algorithm approach for periods of known historical survey data, and compared the distribution of change predicted pixels amongst historically undisturbed areas using a post-hoc analysis. The evolution of NSR disturbances over time were then compared to help to determine the algorithm's applicability for continuous change detection.

2. Study area and data

2.1. Study location

The Quesnel Timber Supply Area (TSA) is located within the Interior Plateau of British Columbia (BC) and characterized by dry forests (annual precipitation of 500–800 mm) and mountainous topography (500—1200 m; Ecological Stratification Working Group, 1995; Hessburg & Agee, 2005). The most common trees in the area include Douglas-fir (*Pseudotsuga menziesii*), lodgepole pine (*Pinus contorta* subsp. *Contorta*), trembling aspen (Populus *tremuloides)* and white spruce (*Picea glacua*). The TSA is divided by the Fraser River, with the area to the west experiencing a drier climate and is more lodgepole Pine dominant, in contrast to the area to the east which receives more rainfall and has more spruce and sub-alpine fir (Ecological Stratification Working Group, 1995). The TSA has experienced significant disturbance over the last 20 years; the largest of these being from wildfires and MPB. Within the TSA,

MPB damage reached its peak around 2005, and by 2009 approximately 68 % of the forest inventory available for harvest at the time was killed (FLNRO, 2016). Wildfires have occurred consistently over the last 10 years with the majority of the impacted areas in the western portion of the TSA. The largest of these fires in 2017, burning approximately 550,000 ha at varying severities (Smith-Tripp et al., 2024). Our study site consists of a 1.4-million-ha area within the eastern portion of the TSA (Fig. 1).

2.2. Moderate resolution satellite imagery

Launched in 1972, Landsat is the longest-running continuous satellite programme, and provides a detailed synoptic and spectrally consistent product at 30 m resolution (Wulder et al., 2022). In 2008 the Landsat archieve was made free and openly available to the public. Combined with advancements in cloud computing and open-source software, there have been significant reduction in barriers to access; making this along with its spectral consistency an appropriate product for this study (Woodcock et al., 2008; Wulder & Coops, 2014).

The Sentinel-2 mission consists of two satellites (S-2A and S-2B) launched in 2015 by the European Space Agency as part of the Copernicus satellite programme (Kempeneers & Soille, 2017). It has a temporal resolution of ≈ 5 days, and 13 spectral bands ranging from 10-60 m spatial resolution (Drusch et al., 2012). Similar to Landsat, Sentinel-2 imagery is open and available for public download and spectrally consistent (Kempeneers & Soille, 2017).

Harmonized Landsat Sentinel-2 (HLS) is a virtual satellite constellation (i.e., combining data from two or more sensors into a single dataset), fusing imagery from Landsat and Sentinel-2 satellites. It is produced in a four step process; (1) Atmospheric correction and cloud masking of both satellites, (2) Geometric resampling and geographic registration, so the product is geometrically consistent, (3) View and illumination angle adjustment using the bidirectional reflectance distribution function (BRDF), which normalizes the solar angle between the satellites, and finally (4) Band Pass Adjustment, which normalizes the spectral bands across sensors (Claverie, et al., 2018). The outcome is a spatially and spectrally consistent data product, with a temporal revisit of 2–3 days at a 30 m spatial resolution (Bolton et al., 2018; Claverie et al., 2018; Mulverhill et al., 2023).

2.3. National terrestrial ecosystem monitoring System (NTEMS)

NTEMS was developed by the Canadian Forest Service to provide a national-scale product for consistent information on disturbance (Hermosilla et al., 2016), and land cover (Hermosilla et al., 2018) for Canada's forested ecosystems using Landsat TM, ETM+, and OLI from 1984 onwards.

Disturbance information uses the Normalized Burn Ratio (NBR; Hermosilla et al., 2016; White et al., 2014) derived from Landsat annual best-available-pixel (BAP) composites. NBR is a spectral index consisting of a normalized difference ratio of near infrared (NIR) to shortwave infrared bands (SWIR), which can be computed from surface reflectance products and has shown to be effective in disturbance detection (Miller et al., 2009). Temporal trends with negative slopes in NBR generally

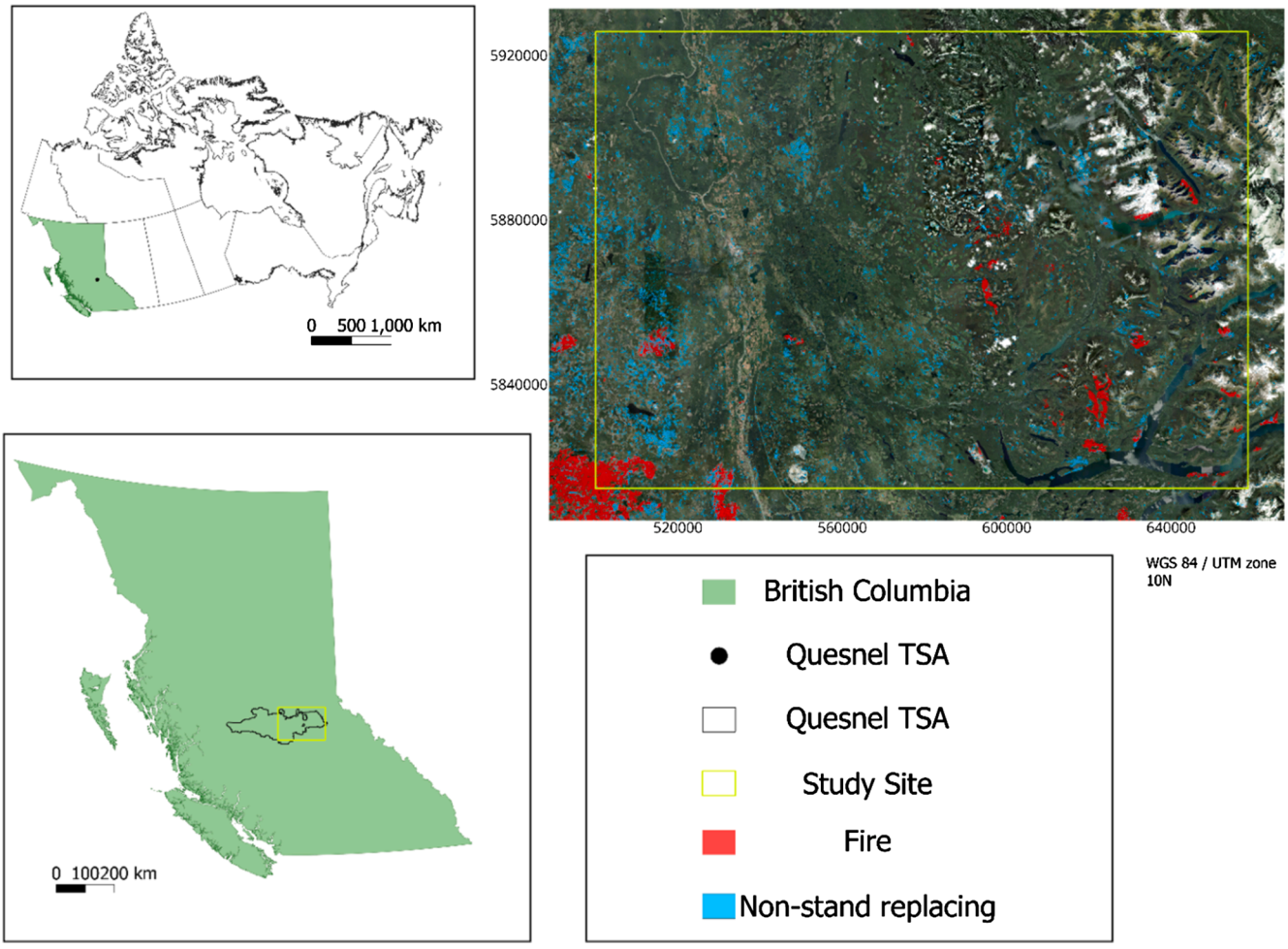

Fig. 1. The study area showing distribution of fire and NSRs from 2002 to 2020. Mapped disturbances derived from Canada's National Terrestrial Ecosystem Monitoring System (Hermosilla et al., 2016).

represent vegetation disturbance (Nguyen et al., 2019; Hermosilla et al., 2015). A hierarchical approach was used to define various change types based on time series metrics (Hermosilla et al., 2015; Hermosilla et al., 2016). Then an object-based analysis utilizing a random forest algoirthm was used to classify individual pixels into change types (i.e., fire, harvesting, road, and non-stand replacing). The NSR category was defined as any disturbance that did not initially result in a land cover change (Hermosilla et al., 2015, 2016). The disturbance detection rates ranged from 96.2 % for harvesting, 95.9 % for fire, 83.5 % for NSR, and 66.3 % for roads (Hermosilla et al., 2016).

National land cover for Canada was produced in Hermosilla et al. (2018) using the Virtual Land Cover Engine (VLCE) framework. Training data was labeled using Earth Observation for Sustainable Development land cover map of forested ecosystems of Canada (Wulder et al., 2008). Next, a Composite2Change approach was applied to determine land cover as one of 11 types, and a Hidden Markov model was used to create logical land cover changes (Hermosilla et al., 2018). The land cover classification layer has an overall accuracy of 70.3 % (Hermosilla et al., 2018).

2.4. British Columbia aerial Overview survey (BC AOS)

The BC AOS is a provincial landscape-level survey used to detect major non-stand replacing disturbances caused by insects, diseases, animals, and abiotic non-anthropogenic factors (Coggins et al., 2008). Aerial surveys have been used in BC since the 1950 s; however, the AOS in its current form has been occurring since 1999 (Coggins et al., 2008; Westfall & Ebata, 2019). The survey flight takes place annually in late July to early September, during leaf-on conditions, in a fixed wing aircraft by experienced observers. The disturbances are classified by intensity, which is defined by percent of the mapped polygon impacted by disturbances that cause mortality (Trace- $<$ 1 %, Light – 1–10 %, Moderate- 11–29 %, Severe- 30–49 %, and Very Severe- $<$ 50 %). For disturbances that do not necessarily cause tree mortality such as defoliation or aspen decline, the disturbance intensity is only categorized from light to severe and defined by reduction in crown foliage (Westfall & Ebata, 2019). The polygons are also attributed with a Forest Health Factor (FHF; i.e., suspected disturbance agent) which falls into categories bark beetle, defoliator, abiotic, diseases, or animals. They are mapped by year as a polygonal dataset (Coggins et al., 2008; Wulder et al., 2006; Westfall & Ebata, 2019).

3. Methods

3.1. Image acquisition and processing

All available Landsat images were downloaded, resampled to the study site, and masked to remove cloud, snow, and water pixels, from January 1st, 2000 – December 31st, 2015 using the Python package *landsatxplore*. HLS v1.4 image (L30 and S30) were downloaded using the *HLS suPER* script from December 31st, 2015 – December 31st, 2020. Upon download, images were already masked and resampled to the study site (Forgett, 2018; NASA, 2024) All imagery was at a 30 m spatial resolution.

NBR values were calculated for every pixel within each image. NBR has been used in national-level change detection protocols in the US and Canada, further suggesting its utility over a broad range of forest types and disturbance regimes (Yang et al., 2018) indicating its practicality for this study. Non-forested pixels based on the NTEMs VLCE were masked and finally, to balance between reducing temporal noise and interfering with the spectral signature, the masked NBR images were mosaiced into 16-day composites, averaging NBR values in each valid pixel, resulting in a total of 228 images (Fig. 2 - 1).

3.2. Algorithm

BEAST utilises the assumption in Bayesian statistics that there are many models for the same series of data and that it is more effective to weigh all these models with varying probabilities rather than trying to find a singular "best-fit" (Banner & Higgs, 2017; Cade, 2015; Zhao et al., 2019). When the algorithm is given a time series of NBR values, seasonality of each pixel is calculated by using a predicted sinusoidal trend, and if a pixel diverges from that sinusoidal trend, it is flagged and a calculated change probability is assigned to the pixel in addition to date at which the change occurred (Mulverhill et al., 2023; Zhao et al., 2019). This allows the algorithm to capture moderate to high-magnitude changes with both positive and negative trajectories suggesting its utility for detecting NSRs, which typically have more variable spatial intensities (Li et al., 2022). The BEAST algorithm was implemented using the *Rbeast* package in R (R Core Team, 2021; Zhao et al., 2019) and run for all images for each year of the study (2002–2020) with additional two years (2000–2001) to spin up the algorithm (i.e., develop the seasonality trend), outputting 19 annual BEAST probability rasters (Fig. 2 - 2).

3.3. BC AOS polygon sampling and NSR summary

The BC AOS polygons from 2000 to 2020 were sampled to extract Moderate, Severe, and Very Severe severity levels. Trace and Light severity level polygons were not used in this study as disturbance areas less than 10 % would be indicative of individual tree decline and typically smaller that the 900 m^2 of a Landsat pixel (Westfall & Ebata, 2019). NSR history within the area was then summarized cumulatively and for individual years of the observation period (2002–2020) (Figs. 2 - 3).

3.4. BEAST probability raster Sampling

BEAST probability rasters were randomly sampled, taking 1,000 pixels from Moderate, Severe, and Very Severe AOS severity levels for each year of the study (2002–2020). This resulted in a total of 44,000 sample pixels, due to Very Severe polygons only occurring in six of the 19 years. Samples of 1,000 pixels were also collected in each year from historically undisturbed areas (regions that had no recorded disturbance during the study period) within each BEAST probability raster, resulting in 19,000 additional sample pixels. Historically undisturbed areas were pixels that did not fall within the AOS survey prior to the year of interest and two years into the future (e.g., for undisturbed areas in 2004, pixels that fell in AOS polygons 2002–2003 and 2005–2006 would be removed from the sample). Additionally, any pixel that was 100 m or less from AOS survey polygons of prior years was removed to account for residual impacts of disturbances (e.g., post-fire windthrow, continued spread of insect infestation, etc.). In total, this resulted in 63,000 NSR and undisturbed sample pixels over the study period (Figs. 2-4).

3.5. Sensitivity of the algorithm to severity level and disturbance agent

A Tukey Honest Significance Difference (HSD) test (Keselman et al., 1977) was applied to the 63,000-pixel sample for each severity level overall, the disturbance agents overall, and the severity level for each individual year in the study. If the severity level or disturbance agent was statistically significant ($p < 0.05$) and higher than the mean value of BEAST of historically undisturbed pixels, BEAST was determined to be detecting the NSR (Figs. 2-5).

The sensitivity of BEAST to disturbance severity level was additionally examined by calculating the overall accuracy of detection. As the BEAST algorithm provides a probability of disturbance rather than a binary classification, a threshold value is required to be calculated to classify the presence of a disturbance event. This threshold was calculated for each severity level individually in addition to a sample of all severity levels using a Receiver Operator Characteristic Curve (ROC)

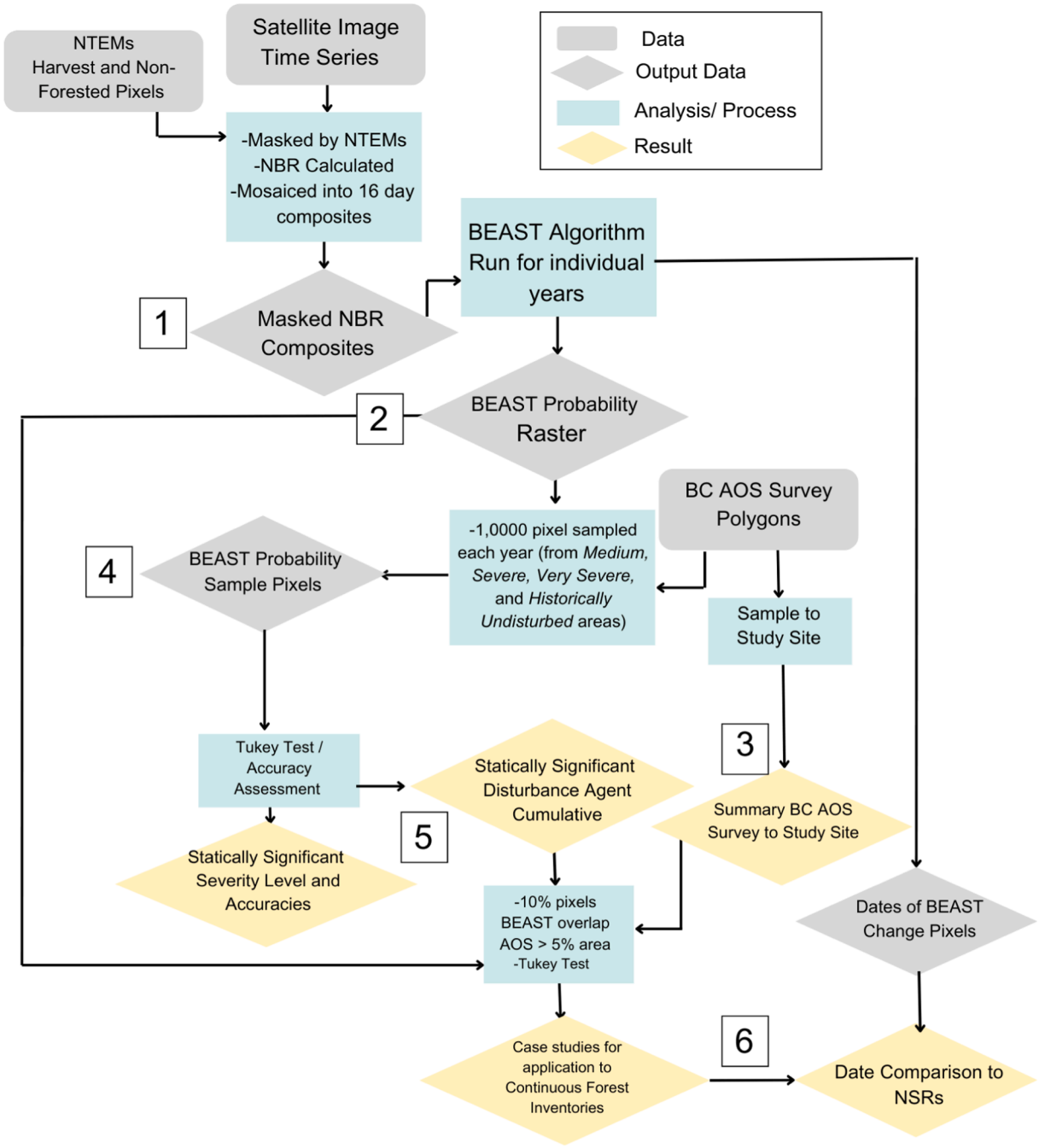

Fig. 2. Methods workflow, (1) Output from Methods *3.1*, (2) Output from Methods *3.2,* (3) Result from Methods *3.3*. (4) Output from Methods *3.4*, (5) Results from Methods *3.5,* and (6) Results from Methods *3.6*.

implemented with the R package *pROC* (LeDell et al., 2015; Robin et al., 2011). BEAST probabilities below the threshold were classified as undisturbed, and probabilities above the threshold were classified as disturbed. Accuracy of detection was then compared across the Undisturbed, Moderate, Severe, Very Severe pixels, and a sample of pixels across all severity levels (Figs. 2–5).

3.6. *Applicability to continuous forest inventories*

In order to determine the algorithm's applicability to a continuous forest inventory, times series analysis of statistically significant, major insect NSRs (> 5 % of total AOS disturbed area) was completed. This was done by combining all years of Moderate, Severe, and Very Severe polygons for each disturbance agent, and taking a 10 % sample of BEAST probability pixels that fell within NSR polygons for consecutive years of disturbance. An HSD Tukey test was then run between all consecutive years. If the algorithm was detecting the progression of an NSR it would be expected that over time, we would expect to see statistically significant ($p < 0.05$) and higher mean value of BEAST probability, indicating the increase of outbreak. The potential application for continuous forest inventories was further examined by comparing the dates at which the BEAST algorithm detected a change and comparing those with a known insect disturbance cycle as a case study (Figs. 2-6).

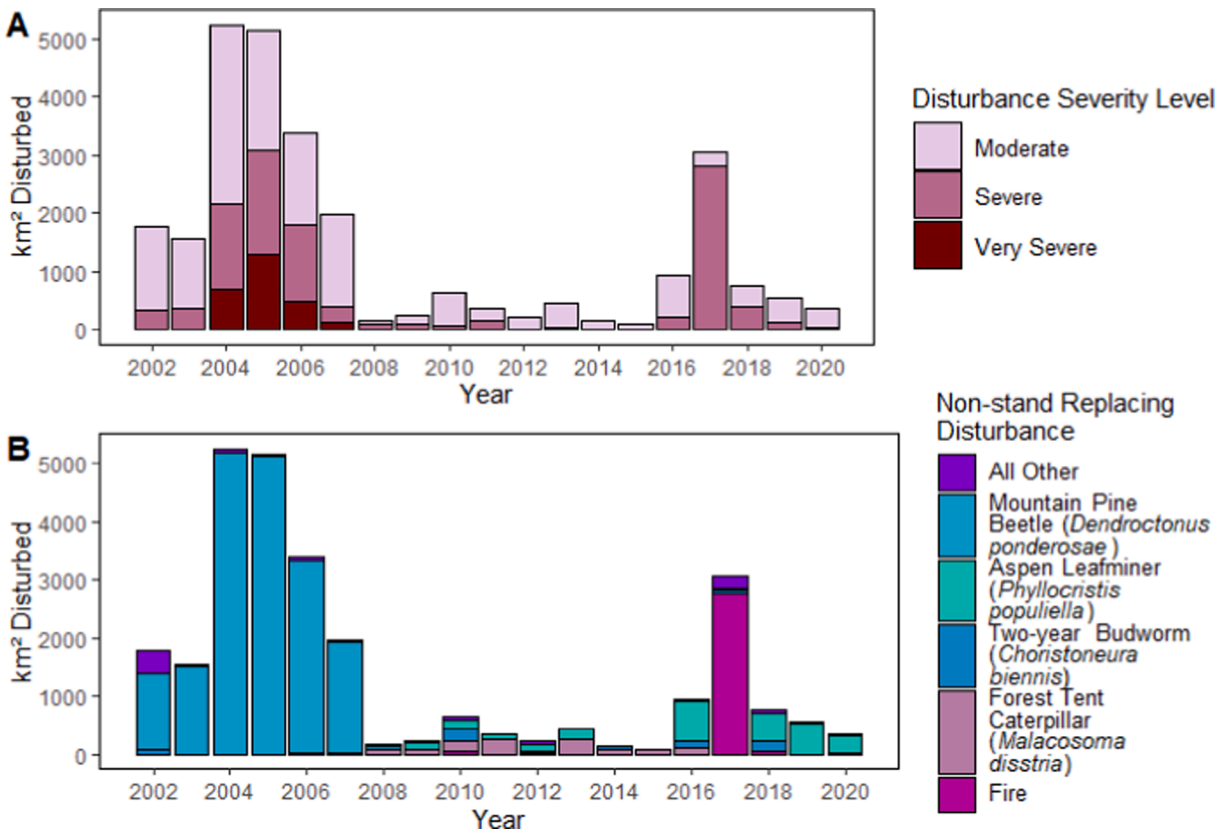

Fig. 3. Km ^{2} of Moderate, Severe, and Very Severe AOS Disturbance from 2002 to 2020, (A) Classified by severity level, and (B) Classified by Disturbance Agent.

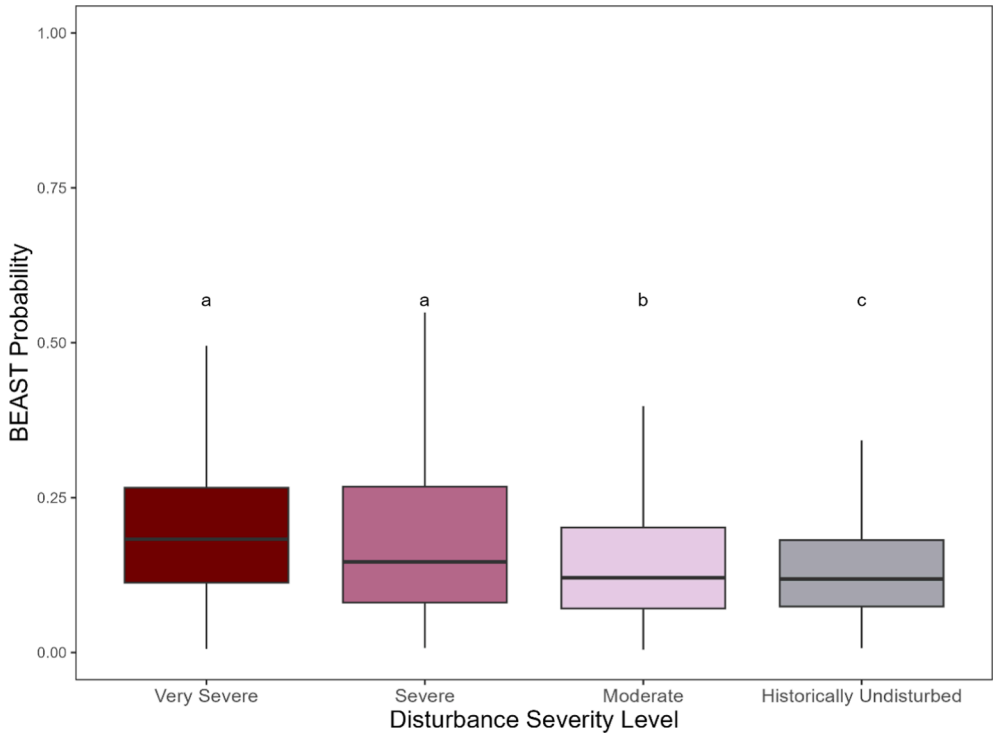

Fig. 4. Distribution of BEAST probability by disturbance severity ($p < 0.05$). Different letters indicate statistically significant differences among categories according to a Tukey HSD test.

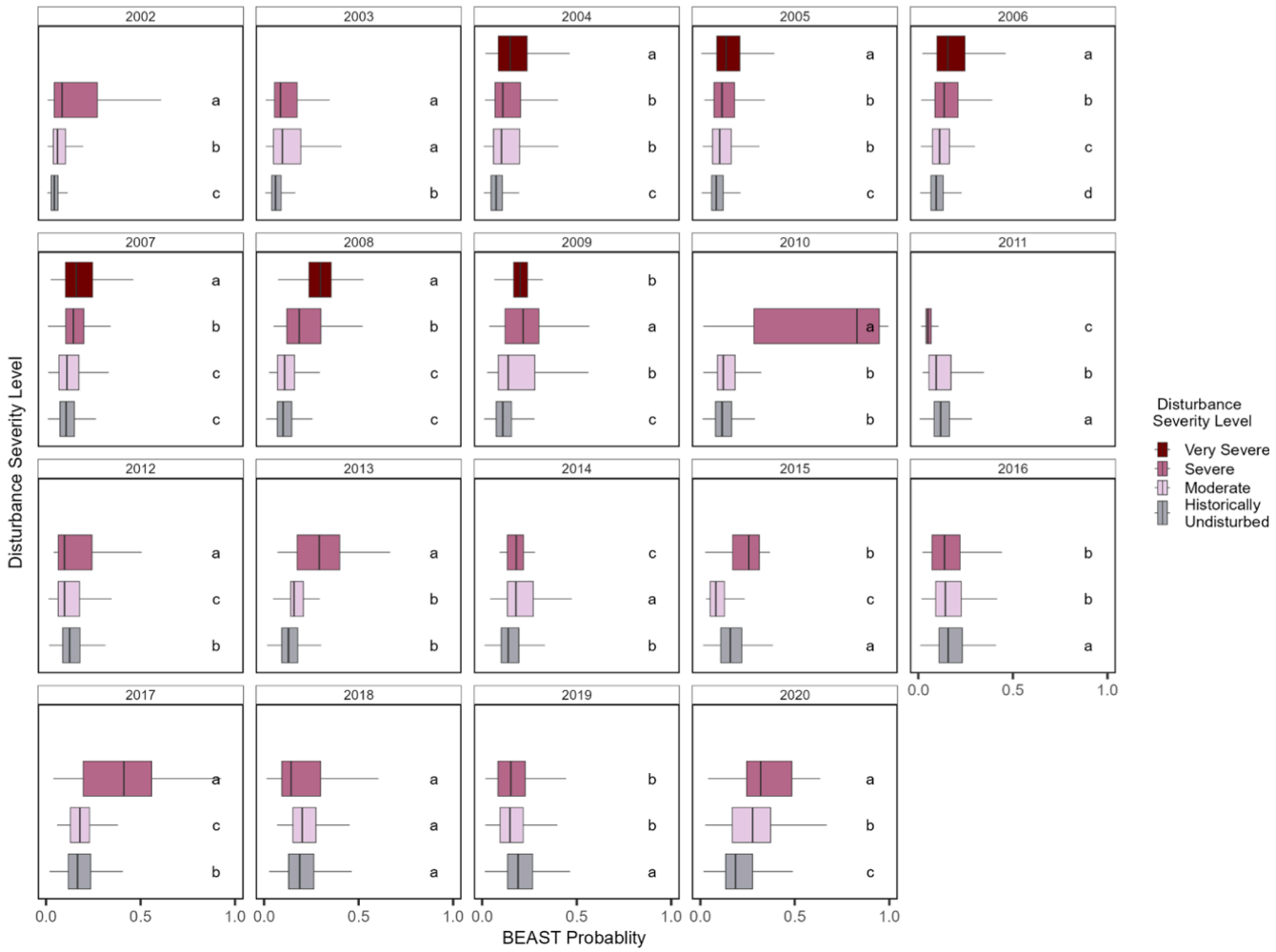

Fig. 5. Distribution of BEAST probability by disturbance severity ($p < 0.05$). Different letters indicate statistically significant differences among categories according to a Tukey HSD test.

4. Results

4.1. Summary of NSRs within the study area

Based on the BC AOS data from 2002 to 2020, the study site experienced ≈ 2.7-million-ha of Moderate, Severe and Very Severe level disturbances from 28 individual disturbance agents, 12 of which made up than < 0.2 % of the total AOS disturbed area (Table 1). Cumulatively ≈ 900,000 ha within the study site (≈ 64 %) had coverage by at least one AOS polygon (many areas were disturbed multiple times). Of these, ≈ 68.1 % of the disturbed area was impacted by MPB occurring between 2002—2008, ≈ 10.7 % was non-stand replacing wildfire, with a smaller proportion of other disturbances (i.e., ≈ 9.8 % Aspen Leafminer (Phyllocnistis populiella), ≈ 4.3 % – Forest Tent Caterpillar (*Malacosoma disstria*), and ≈ 2.9 % Two-year Budworm (*Choristoneura biennis*); Westfall & Ebata, 2019; Fig. 3).

4.2. Sensitivity to disturbance severity level

When compared across all years cumulatively (2002–2020) Moderate, Severe, and Very Severe classified pixels all had higher and statistically significant ($p < 0.05$) BEAST mean change probabilities of 0.155, 0.203, and 0.202, respectively, when compared with historically undisturbed pixels that had a mean probability of 0.119 (Fig. 4). With respect to the sensitivity of the BEAST algorithm to different severity levels, Moderate severity disturbances were significantly lower than Severe and Very Severe disturbances, but the latter two were not statistically significantly difference from each other (Fig. 4). When individual years (2002–2020) were compared, Very Severe disturbances were significantly higher than historically undisturbed pixels in all six years in which they occurred (i.e., 2004–2009) whereas the Severe disturbance category was significantly higher than historically undisturbed pixels in 13 of the 19 years of the study (i.e., 2002–2010, 2012, 2013, 2017, 2020). Moderate severity disturbance was less well discriminated amongst years, with statistically significant differences being detected in eight of the 19 years within the study (i.e., 2002–2006, 2009, 2014, 2020; Fig. 5). The five highest disturbance years (2002, 2004, 2005, 2006, and 2017), which together made up ≈ 69.5 % of the total combined AOS disturbed area and all (with the exception of Moderate severity level in 2017) had probabilities significantly higher than those of historically undisturbed pixels (Fig. 5). The Overall, Producer's and User's accuracies of each severity level were mostly in accordance with this trend with respective accuracies of; Very Severe – 64.3 %, 62.4 % and 64.8 %, Severe- 58.3 %, 34.2 % and 66.0 %, and Moderate 52.5 %., 22.5 % and 56.3 %, respectively (Table 2).

4.3. Sensitivity to disturbance agent

In total there were 28 different disturbance agents mapped by the AOS survey during the study period (2002–2020). Sixteen of the 28 had significantly higher ($p < 0.05$) mean values compared to the mean BEAST probability value of 0.144 for historically undisturbed pixels (i.

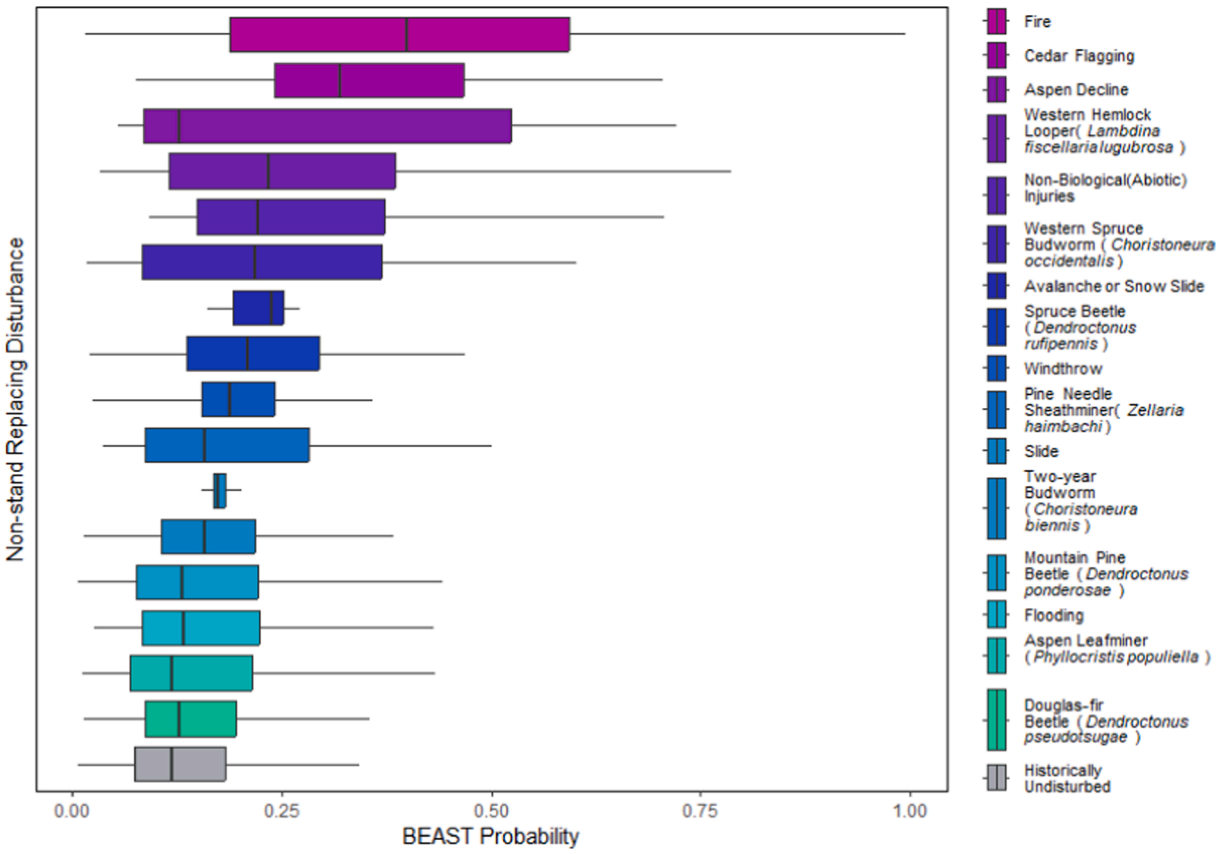

Fig. 6. Disturbance Agents from 2002 −2020 with significantly higher ($p < 0.05$) mean BEAST probability values when compared to Historically Undisturbed pixels in the order of mean BEAST probability value highest (top) and lowest (bottom).

Table 1
Table of disturbance agents (<0.2 % of AOS disturbed area).

Disturbance Agent	% Of AOS Disturbed Area
Mountain Pine Beetle (*Dendroctonus ponderosae*)	68.1
Fire	10.7
Aspen Leafminer (*Phyllocristis populiella*)	9.8
Forest Tent Caterpillar (*Malacosoma disstria*)	4.3
Two-year Budworm (*Choristoneura biennis*)	2.9
Satin Moth (*Leucoma salicis*)	0.9
Western Hemlock Looper (*Lambdina fiscellaria lugubrosa*)	0.6
Spruce Beetle (*Dendroctonus rufipennis*)	0.6
Douglas-fir Beetle (*Dendroctonus pseudotsugae*)	0.5
Western Balsam Bark Beetle (*Dryocoetes confusus*)	0.4
Dothistroma needle blight	0.3
Windthrow	0.2
Western Winter Moth (*Erranis tiliaria vancouverensis*)	0.2
Cedar Flagging	0.2
Pine Needle Sheathminer (*Zellaria haimbachi*)	0.2

e., Douglas Fir Beetle – 0.154, MPB – 0.164, Spruce Beetle – 0.214, Aspen Leafminer – 0.158, Two- year Budworm – 0.172, Pine Needle Sheathminer – 0.186, Western Hemlock Looper – 0.280, Western Spruce Budworm – 0.230, Non-biological Injuries – 0.275, Avalanche or Snowslide – 0.226, Fire – 0.427, Aspen Decline – 0.287, Cedar Flagging – 0.350, Slide – 0.179, and Windthrow – 0. 197; Fig. 6). These 16 disturbance agents made up ≈ 93.9 % of the total AOS mapped disturbances by area within the study. Of these 16 detectable disturbances, four (i.e., Mountain Pine Beetle, Fire (non-stand replacing), Aspen Leafminer and Two-year Budworm) of the five disturbance agents that made up more than 2.5 % of the AOS survey data individually and together making up 91.5 % by area of all AOS survey data cumulatively were all detectable.

4.4. Applicability to continuous forest inventories

In order to assess the BEAST algorithms applicability to continuous forest inventories, BEAST probability values from the two largest insect disturbances by area (i.e., MPB, and Aspen Leafminer) were compared to their respective AOS mapped areas. Then MPB, due to its epidemic levels reached in the early 2000 s, had a particularly well documented lifecycle history and was compared to known markers in the species lifecycle to further assess the algorithms application for continuous forest inventories.

4.4.1. Aspen Leafminer

Aspen Leafminer was the second largest insect disturbance in the

Table 2
Estimated accuracies of method at varying disturbance severities.

Severity Level	Producer's Accuracy %	User's Accuracy %	Error of Omission %	Error of Commission %	Overall Accuracy %
Very Severe	62.4	64.8	37.6	33.8	64.3
Severe	34.2	66.0	65.8	17.7	58.3
Moderate	22.5	56.3	77.5	17.5	52.5
All Severity Levels	30.5	62.9	69.5	18.0	56.3

study site with ≈ 9.8 % of the total AOS disturbed area. Aspen Leafminer was mapped sporadically during the 2009–2020 period, with the highest years by area being 2016, 2018, and 2019 with 68,298, 46,438, and 53,222 ha impacted, respectively. The differences in BEAST probability value distributions were examined for Aspen Leafminer impacted areas from 2016 to 2020. In 2016, there was a mean BEAST probability of change value with all polygons of 0.160 which increased to 0.185 in 2020 (2017—0.163, 2018—0.178, 2019—0.182, 2020 – 0.185). Years 2016–2019 were significantly ($p < 0.05$) different from each other. This increasing progression of BEAST probability detected values corresponded to increases in cumulative Aspen Leafminer impact from 2016 to 2020 (Fig. 7).

4.4.2. Mountain Pine Beetle (MPB)

MPB overall was the largest disturbance in the study site with ≈ 68.1 % of the total AOS disturbed area. MPB was mapped from 2002 to 2008, with 131,800, 149,700, 516,534, 511,820, 330,227, 195,000, and 70,000 ha impacted in each year, respectively. The differences in BEAST probability value distributions were examined for MPB impacted areas from 2002 to 2008. In 2002, there was a mean BEAST probability of change value for all polygons of 0.065, which increased to 0.347 in 2008 (2003—0.101, 2004—0.155, 2005—0.253, 2006—0.309, 2007 – 0.330, 2008—0.347). All years were significantly ($p < 0.05$) different from each other. This upwards progression of BEAST probability detected values was correspondent to the cumulative MPB impact from 2002 to 2008 (Fig. 8).

Additionally, BEAST recorded the date at which at individual pixel experienced a change and the disturbed area could be calculated from this. From 2002 to 2008, the lowest change months for each year were all in the winter and late fall i.e., January 2002 (837 ha), December 2003 (1,014 ha), January 2004 (1,005 ha), February 2005 (2,155 ha) December 2006 (1,351 ha), January 2007 (1,333 ha), and November 2008 (956 ha). The highest change months for each year were mostly in the spring or early fall (i.e., April 2002 (8,484 ha), April 2003 (50,577 ha), September 2004 (23,306 ha), April 2005 (64,913 ha), September 2006 (23,063 ha), and May 2007 (18,598 ha), and April 2008 (23, 829 ha; Fig. 9).

5. Discussion

5.1. Sensitivity to severity and disturbance agent

Across all years combined, the BEAST algorithm had a statistically significant detection ($p < 0.05$) of Moderate, Severe, and Very Severe disturbances. However, amongst individual years, the algorithm was not always able to successfully detect Severe and Moderate level disturbances, detecting 13 of 19 years and eight of 19 years, respectively. In years where disturbed pixels were not well discriminated from historically undisturbed pixels (i.e., 2011, 2015, 2016, 2018, 2019), overall disturbances tended to be lower across the landscape only composing 12.9 % of AOS disturbed area and with most prevalent disturbance agents being *Forest Tent Caterpillar* at 23.0 % of the AOS disturbance area, which the BEAST algorithm did not detect at a statistically significant level ($p < 0.05$). All severity levels had moderate accuracies – which in part may be due to the assumption that 100 % of the pixels that fell with an AOS polygon were disturbed at the visually determined severity level. Studies have found that there is a range of disturbance severities within AOS polygons (Westfall & Ebata, 2019; Coggins et al., 2008) making exact correspondence between the AOS and BEAST disturbance severity levels more challenging.

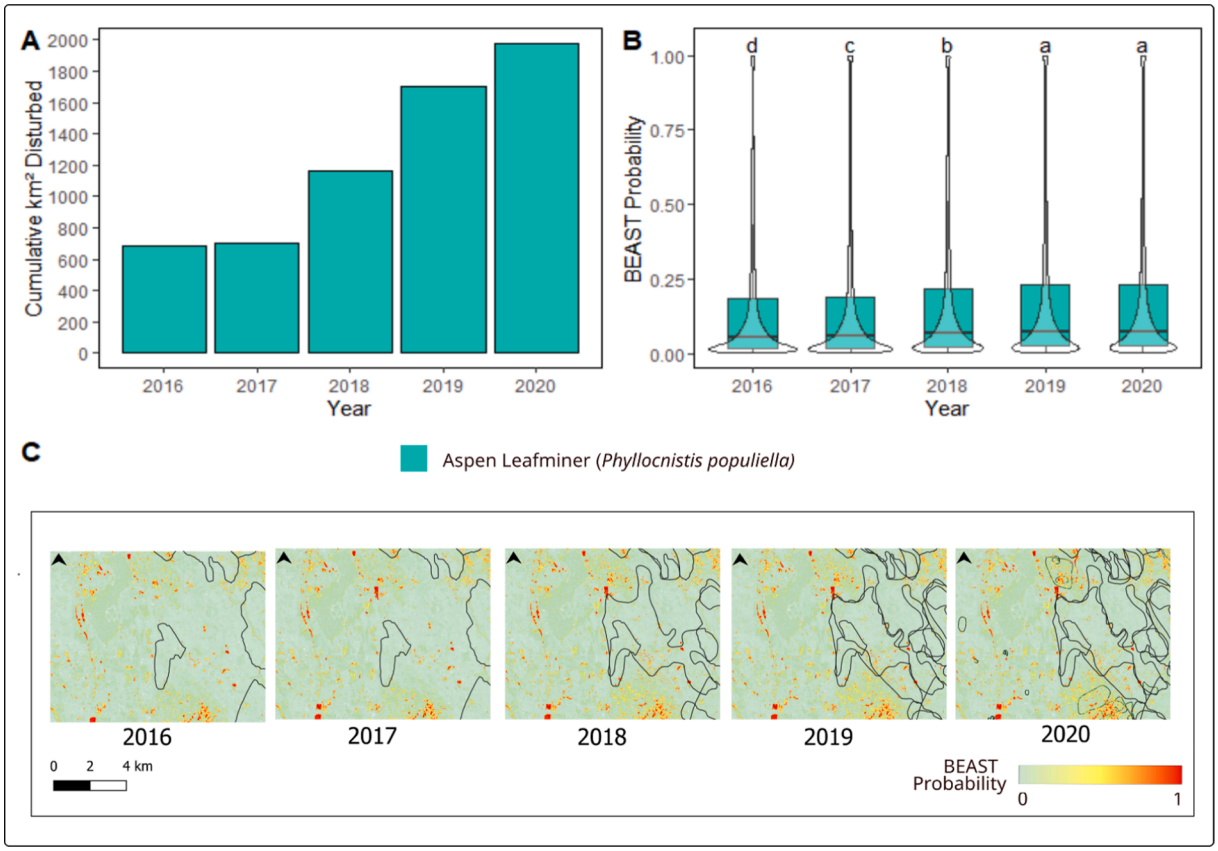

Fig. 7. (A) Cumulative Moderate, Severe, and Very Severe Aspen Leafminer disturbance (2016–2020), (B) Aspen Leafminer BEAST probability values by year ($P < 0.05$). Different letters indicate statistically significant differences among years according to a Tukey HSD test. (C) Example area of BEAST Aspen Leafminer detection (2016–2020) with corresponding BC AOS polygons in black.

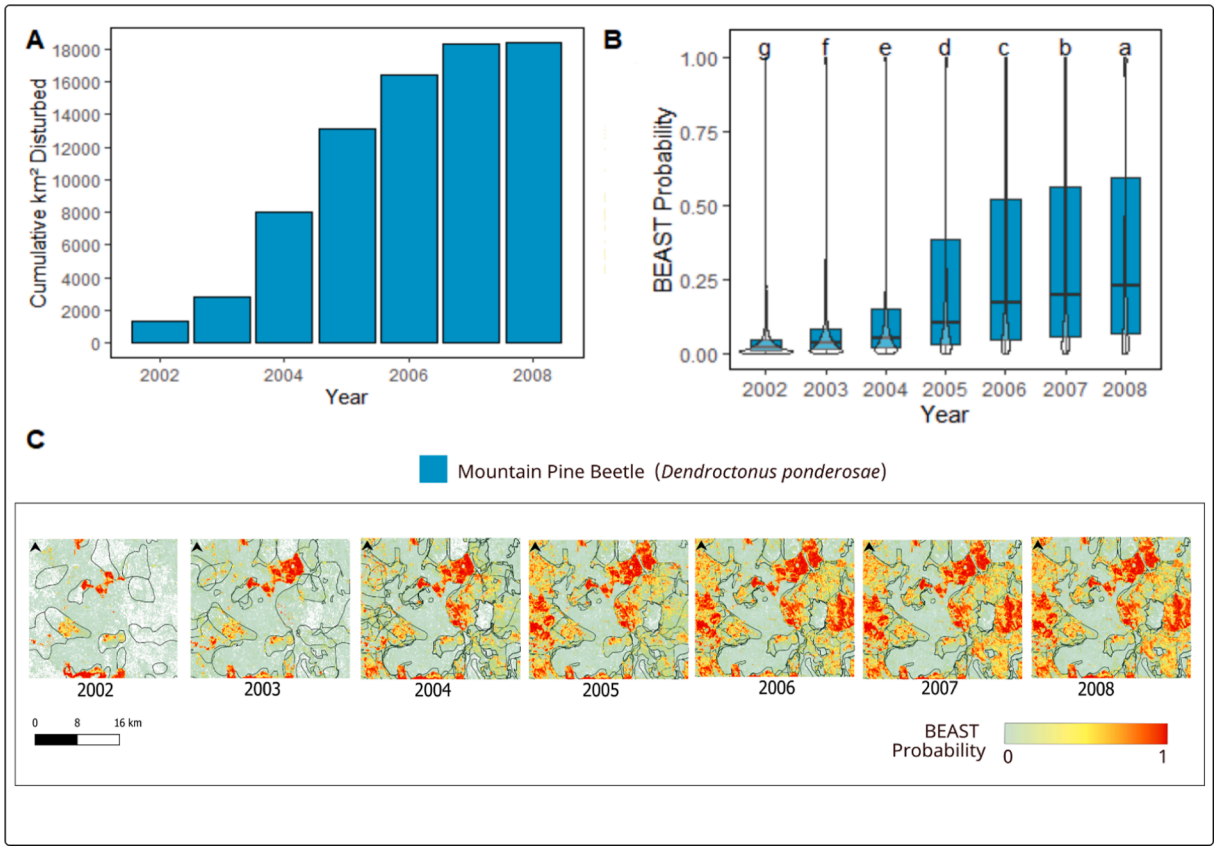

Fig. 8. (A) Cumulative Moderate, Severe, and Very Severe MPB disturbance (2002–2008), (B) MPB BEAST Probability by year ($P < 0.05$), (C) Example area of BEAST MPB detection) with corresponding BC AOS polygons in black (2002–2006). Different letters indicate statistically significant differences among years according to a Tukey HSD test.

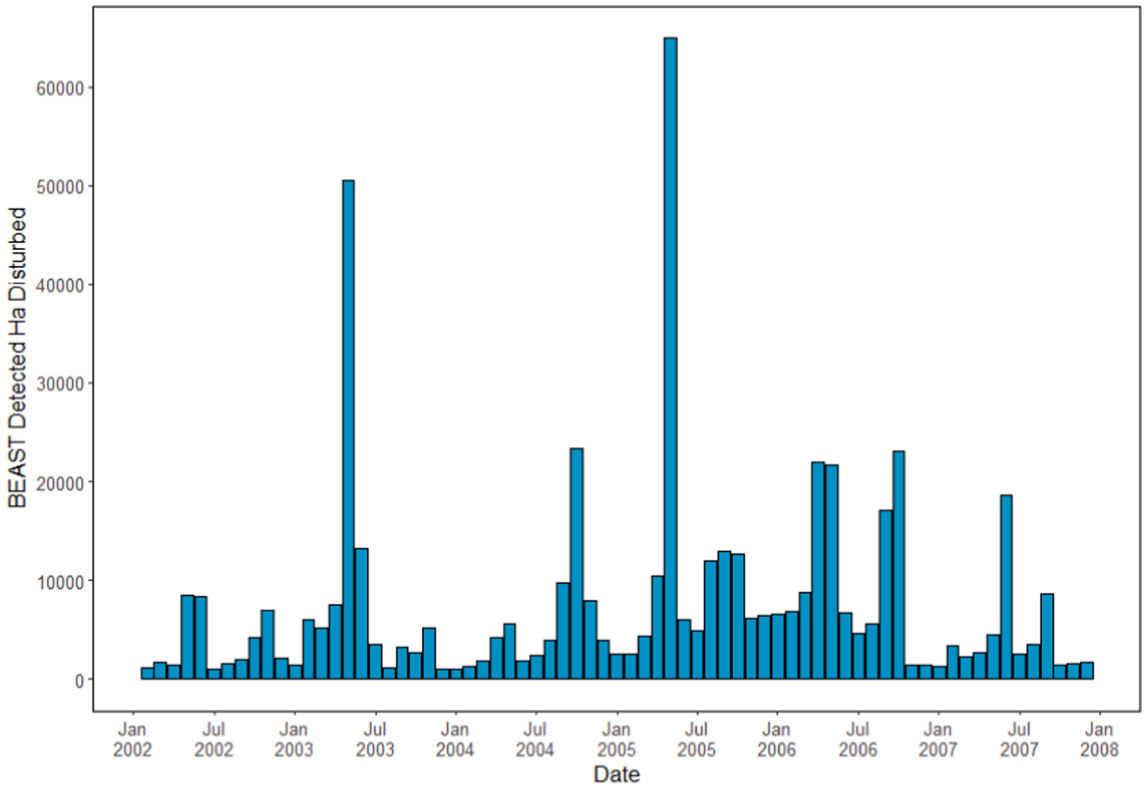

Fig. 9. Area BEAST detected disturbance over time (2002–2008) in hectares within MPB surveyed area.

Overall, the BEAST algorithm performed well, capturing 16 types of NSRs comprising ≈ 93.9 % of the AOS survey polygon by area. BEAST did particularly well with NSRs that lead to some level of mortality, showing statistically significant values for three of the four bark beetles (i.e., Douglas Fir Beetle, MPB, and Spruce Beetle). This made up ≈ 99.4 % of the bark beetle disturbance by survey area. Seven of the 11 abiotic disturbances (i.e., Non-biological Injuries, Avalanche or Snowslide, Fire, Aspen Decline, Cedar Flagging, Slide, and Windthrow) were also detected which made up ≈ 99.6 % of the abiotic disturbance by AOS survey area. The algorithm was less successful at capturing disturbances that do not individually cause mortality such as defoliators. The algorithm captured six of the ten defoliators (i.e., Aspen Leafminer, Two-year Budworm, Pine Sheathminer, Western Hemlock Looper, and Western Spruce Budworm) which made up ≈72.0 % of the defoliator disturbances by AOS survey area. The 28.0 % of defoliators which the BEAST algorithm was not sensitive to mostly consisted of Forest Tent Caterpillar at 23.0 %, and 4.97 % Satin Moth *(Lepidoptera Lymanriidae)* with small percentages of Large Aspen Tortrix (Choristoneura conflictana) and Unspecified Defoliator. The algorithm did not show sensitivity in capturing diseases during the study period (i.e., Needle Blight (Dothistroma septosporum) and Pine Needle Cast (Lophodermella concolor); however, disease made up only 0.33 % of all surveyed disturbances.

The BEAST algorithm's inability to capture all disturbances may be linked to the sensitivity of NBR to some NSR disturbances. We selected NBR due to its broad utility for disturbance detection, and a documented history of sensitivity over a wide range of forest types and disturbance regimes (Alcaras et al., 2022; White et al., 2017). That said, NBR was initially developed to capture burned area post wildfire by detecting the colour shift from green healthy vegetation to brown vegetation (Yang et al., 2018). However, many defoliators and disease do not necessarily cause vegetation to transition from green to brown, but are more likely to lead to a change in overall productivity and canopy cover (Castagneri et al., 2020). For instance, the *Forest Tent Caterpillar* strips foliage away from trees which leads to lower rates of photosynthesis and in turn a loss in productivity and moisture content (Hall et al., 2016). To further assess the BEAST algorithm's sensitivity to defoliators additional indices that capture vegetation greenness or moisture content such as Normalized Difference Vegetation Index (NDVI), Tasseled Cap Greenness (TCG), Normalized Difference Moisture Index (NDMI), or Tasseled Cap Wetness (TCW; Hall et al., 2016; Pasquarella et al., 2017; Pasquarella et al., 2021) could be considered.

5.2. Applicability to continuous forest inventories

As the BC AOS is an annual survey, it is not possible to determine the exact utility to sub-annual detectability. However, as progressive outbreak periods were captured when observed at the annual timestep with the use of 16-day composite images, there is demonstrated potential in the BEAST algorithm's ability to detect NSRs at a sub-annual timescale. This is further illustrated when BEAST detection dates were compared to the life cycle of MPB in the epidemic stage (Carroll et al., 2004; Perez., 2009; Safranyik et al., 2010).

MPB has a relatively well documented life cycle, particularly at the epidemic level as it was in the region from 2002 to 2008 (Safranyik et al., 2010). The pupa emerges as adults in the spring and early summer. Then, they subsequently find and attack new trees in the summer/early fall, with attack ceasing in mid fall with the arrival of freezing conditions as individuals have entered trees and laid eggs (Carroll et al., 2004; Perez., 2009; Safranyik et al., 2010). The BEAST algorithm's transition corresponded well to the anticipated cycle of attack, demonstrating spikes of changes in the spring as trees are initially attacked and then again around September-October, with a drop shortly after associated with cooling temperatures (first freeze in Quesnel is generally around mid- September; Environment and Climate Change Canada, 2024).

5.3. Future considerations

Our results suggest that the BEAST algorithm has the potential to detect a range of NSRs at a variety of severity levels, and is likely to be able to monitor these changes at sub-annual time intervals. However, as the impact on forest structure greatly varies by disturbance, to conceptualize forest structural impact from continuously detected BEAST outputs, there is a need to further spectrally characterize the disturbance type (Coops et al., 2020; Varhola et al., 2010). For instance, a defoliator may reduce canopy cover, whereas mechanical disturbances such as non-stand replacing fire would cause some trees to fall, thereby reducing mean canopy height. Once disturbance agents are identified with a sufficient degree of confidence, field campaigns for further validation, targeted acquisitions of remotely piloted aerial systems (RPAs) or aircraft-based images or LiDAR data may be planned and implemented to provide more detailed information on the structural effects of disturbances (Coops et al., 2020).

6. Conclusion

Detecting NSRs is fundamental to any continuous forest inventory framework (Coops et al., 2023). NSRs often lead to more variable stand structures than stand-replacing disturbances (Peng et al., 2011), and can greatly impact both timber supply and forest ecosystem services. Additionally, NSRs frequently act as a key driver of forest composition shifts and biomass dynamics, making them critical to consider when anticipating the future condition of a forest (Payette et al. 1990; Woods 2000; Woods and Kern 2022; Morin-Bernard et al., 2023). Our results demonstrated that the developed approach showed potential to detect a variety of NSR types at differing severity levels, in addition to detecting the progression of two major insect disturbances. This study therefore suggests the potential of our methodology to better quantify the impacts caused by NSRs under a changing climate.

CRediT authorship contribution statement

Madison S. Brown: Writing – review & editing, Writing – original draft, Visualization, Methodology, Formal analysis, Data curation, Conceptualization. **Nicholas C. Coops:** Writing – review & editing, Writing – original draft, Supervision, Methodology, Funding acquisition, Conceptualization. **Christopher Mulverhill:** Writing – review & editing, Writing – original draft, Methodology, Conceptualization. **Alexis Achim:** Writing – review & editing, Writing – original draft, Methodology, Funding acquisition, Conceptualization.

Declaration of competing interest

The authors declare that they have no known competing financial interests or personal relationships that could have appeared to influence the work reported in this paper.

Acknowledgements

This analysis was conducted on the ancestral and unceded territories of the xʷməθkʷəy̓əm (Musqueam), Dënéndeh and Tsílhqot'in Nen people. This research was funded by a NSERC Alliance project Silva21 NSERC ALLRP 556265 – 20, grantee Prof. Alexis Achim. We thank the anonymous reviewers whose feedback helped to improve and clarify this manuscript.

References

Achim, A., Moreau, G., Coops, N.C., Axelson, J.N., Barrette, J., Bédard, S., Byrne, K.E., Caspersen, J., Dick, A.R., D'Orangeville, L., Drolet, G., Eskelson, B.N.I., Filipescu, C. N., Flamand-Hubert, M., Goodbody, T.R.H., Griess, V.C., Hagerman, S.M., Keys, K., Lafleur, B., White, J.C., 2022. The changing culture of silviculture. *Forestry: an*

International Journal of Forest Research 95 (2), 143–152. https://doi.org/10.1093/forestry/cpab047.
Agee, J. K. (1993). *Fire Ecology of Pacific Northwest Forests*.
Alcaras, E., Costantino, D., Guastaferro, F., Parente, C., Pepe, M., 2022. Normalized Burn Ratio Plus (NBR+): a new index for sentinel-2 imagery. Remote Sens. (Basel) 14 (7), 1727. https://doi.org/10.3390/rs14071727.
Banner, K.M., Higgs, M.D., 2017. Considerations for assessing model averaging of regression coefficients. *Ecol. Appl.* 27 (1), 78–93. https://doi.org/10.1002/eap.1419.
Bender, E.A., Case, T.J., Gilpin, M.E., 1984. Perturbation experiments in community ecology—theory and practice. Ecology 65, 1–13.
Bigler, C., Kulakowski, D., Veblen, T.T., 2005. Multiple disturbance interactions and drought influence fire severity in Rocky Mountain subalpine forests. Ecology 86, 3018–3029. https://doi.org/10.1890/05-0011.
Bolton, D.K., White, J.C., Wulder, M.A., Coops, N.C., Hermosilla, T., Yuan, X., 2018. Updating stand-level forest inventories using airborne laser scanning and Landsat time series data. *Int. J. Appl. Earth Obs. Geoinf.* 66, 174–183. https://doi.org/10.1016/j.jag.2017.11.016.
Bontemps, J.-D., Bouriaud, O., Vega, C., Bouriaud, L., 2022. Offering the appetite for the monitoring of European forests a diversified diet. *Ann. For. Sci.* 79 (1), 19. https://doi.org/10.1186/s13595-022-01139-7.
Brown, M., Black, T.A., Nesic, Z., Foord, V.N., Spittlehouse, D.L., Fredeen, A.L., Grant, N. J., Burton, P.J., Trofymow, J.A., 2010. Impact of mountain pine beetle on the net ecosystem production of lodgepole pine stands in British Columbia. *Agric. For. Meteorol.* 150 (2), 254–264. https://doi.org/10.1016/j.agrformet.2009.11.008.
Cade, B.S., 2015. Model averaging and muddled multimodel inferences. *Ecology* 96 (9), 2370–2382. https://doi.org/10.1890/14-1639.1.
Carroll, A. L., Taylor, S. W., Régnière, J., & Safranyik, L. (2004). *Effects of Climate Change on Range Expansion by the Mountain Pine Beetle in British Columbia*.
Castagneri, D., Prendin, A.L., Peters, R.L., Carrer, M., von Arx, G., Fonti, P., 2020. Long-term impacts of defoliator outbreaks on larch xylem structure and tree-ring biomass. Front. Plant Sci. 11, 1078. https://doi.org/10.3389/fpls.2020.01078.
Chen, N., Tsendbazar, N.-E., Hamunyela, E., Verbesselt, J., Herold, M., 2021. Sub-annual tropical forest disturbance monitoring using harmonized Landsat and Sentinel-2 data. *Int. J. Appl. Earth Obs. Geoinf.* 102, 102386. https://doi.org/10.1016/j.jag.2021.102386.
Claverie, M., Ju, J., Masek, J.G., Dungan, J.L., Vermote, E.F., Roger, J.-C., Skakun, S.V., Justice, C., 2018. The Harmonized Landsat and Sentinel-2 surface reflectance data set. *Remote Sens. Environ.* 219, 145–161. https://doi.org/10.1016/j.rse.2018.09.002.
Coggins, S.B., Wulder, M.A., Coops, N.C., White, J.C., 2008. Linking survey detection accuracy with ability to mitigate populations of mountain pine beetle. *For. Chron.* 84 (6), 900–909. https://doi.org/10.5558/tfc84900-6.
Cohen, W.B., Yang, Z., Stehman, S.V., Schroeder, T.A., Bell, D.M., Masek, J.G., Huang, C., Meigs, G.W., 2016. Forest disturbance across the conterminous United States from 1985–2012: The emerging dominance of forest decline. *For. Ecol. Manage.* 360, 242–252. https://doi.org/10.1016/j.foreco.2015.10.042.
Coops, N.C., Johnson, M., Wulder, M.A., White, J.C., 2006. Assessment of QuickBird high spatial resolution imagery to detect red attack damage due to mountain pine beetle infestation. *Remote Sens. Environ.* 103 (1), 67–80. https://doi.org/10.1016/j.rse.2006.03.012.
Coops, N.C., Wulder, M.A., Duro, D.C., Han, T., Berry, S., 2008. The development of a Canadian dynamic habitat index using multi-temporal satellite estimates of canopy light absorbance. Ecol. Ind. 8 (5), 754–766. https://doi.org/10.1016/j.ecolind.2008.01.007.
Coops, N.C., Shang, C., Wulder, M.A., White, J.C., Hermosilla, T., 2020. Change in forest condition: Characterizing non-stand replacing disturbances using time series satellite imagery. *For. Ecol. Manage.* 474, 118370. https://doi.org/10.1016/j.foreco.2020.118370.
Coops, N.C., Tompalski, P., Goodbody, T.R.H., Achim, A., Mulverhill, C., 2023. Framework for near real-time forest inventory using multi source remote sensing data. *Forestry: an International Journal of Forest Research* 96 (1), 1–19. https://doi.org/10.1093/forestry/cpac015.
Culvenor, D., Newnham, G., Mellor, A., Sims, N., Haywood, A., 2014. Automated in-situ laser scanner for monitoring forest leaf area index. *Sensors* 14 (8), 14994–15008. https://doi.org/10.3390/s140814994.
DeRose, R.J., Long, J.N., Ramsey, R.D., 2011. Combining dendrochronological data and the disturbance index to assess Engelmann spruce mortality caused by a spruce beetle outbreak in southern Utah, USA. *Remote Sens. Environ.* 115 (9), 2342–2349. https://doi.org/10.1016/j.rse.2011.04.034.
Drusch, M., Del Bello, U., Carlier, S., Colin, O., Fernandez, V., Gascon, F., Hoersch, B., Isola, C., Laberinti, P., Martimort, P., Meygret, A., Spoto, F., Sy, O., Marchese, F., Bargellini, P., 2012. Sentinel-2: ESA's optical high-resolution mission for GMES operational services. *Remote Sens. Environ.* 120, 25–36. https://doi.org/10.1016/j.rse.2011.11.026.
Ecological Stratification Working Group. (1995). *A national ecological framework for Canada*. Centre for Land and Biological Resources Research, Research Branch, Agriculture and Agri-Food Canada.
Environment and Climate Change Canada. (2024). Climate data - Historical data - Quesnel. https://climate.weather.gc.ca/historical_data/search_historical_data.
BC Ministry of Forests, Land, and Natural Resource Operations (FLNRO). (2016). Quesnel Timber Supply Area Timber Supply Analysis Discussion Paper. Forest Analysis and Inventory Branch, Ministry of Forests, Lands, and Natural Resource Operations.
Forget, Y. (2023). Landsatxplore (1.0.3) [Software]. PyPI. https://pypi.org/project/landsatxplore/.
Franklin, S.E., Fan, H., Guo, X., 2008. Relationship between Landsat TM and SPOT vegetation indices and cumulative spruce budworm defoliation. *Int. J. Remote Sens.* 29 (4), 1215–1220. https://doi.org/10.1080/01431160701730136.
Giannetti, F., Pecchi, M., Travaglini, D., Francini, S., D'Amico, G., Vangi, E., Cocozza, C., Chirici, G., 2021. Estimating VAIA windstorm damaged forest area in italy using time series sentinel-2 imagery and continuous change detection algorithms. *Forests* 12 (6), 680. https://doi.org/10.3390/f12060680.
Gillis, M.D., Leckie, D.G., 1996. Forest inventory update in Canada. *The For. Chron.* 72 (2), 138–156. https://doi.org/10.5558/tfc72138-2.
Goodwin, N.R., Magnussen, S., Coops, N.C., Wulder, M.A., 2010. Curve fitting of time-series Landsat imagery for characterizing a mountain pine beetle infestation. *Int. J. Remote Sens.* 31 (12), 3263–3271. https://doi.org/10.1080/01431160903186277.
Hall, R.J., Castilla, G., White, J.C., Cooke, B.J., Skakun, R.S., 2016. Remote sensing of forest pest damage: A review and lessons learned from a Canadian perspective. The Can. Entomol. 148 (S1), S296–S356. https://doi.org/10.4039/tce.2016.11.
Hansen, M.C., Loveland, T.R., 2012. A review of large area monitoring of land cover change using Landsat data. *Remote Sens. Environ.* 122, 66–74. https://doi.org/10.1016/j.rse.2011.08.024.
Hermosilla, T., Wulder, M.A., White, J.C., Coops, N.C., Hobart, G.W., 2015. Regional detection, characterization, and attribution of annual forest change from 1984 to 2012 using Landsat-derived time-series metrics. *Remote Sens. Environ.* 170, 121–132. https://doi.org/10.1016/j.rse.2015.09.004.
Hermosilla, T., Wulder, M.A., White, J.C., Coops, N.C., Hobart, G.W., Campbell, L.B., 2016. Mass data processing of time series Landsat imagery: Pixels to data products for forest monitoring. *Int. J. Digital Earth* 9 (11), 1035–1054. https://doi.org/10.1080/17538947.2016.1187673.
Hermosilla, T., Wulder, M.A., White, J.C., Coops, N.C., Hobart, G.W., 2018. Disturbance-informed annual land cover classification maps of canada's forested ecosystems for a 29-year landsat time series. *Can. J. Remote. Sens.* 44 (1), 67–87. https://doi.org/10.1080/07038992.2018.1437719.
Hermosilla, T., Wulder, M.A., White, J.C., Coops, N.C., 2019. Prevalence of multiple forest disturbances and impact on vegetation regrowth from interannual Landsat time series (1985–2015). Remote Sens. Environ. 233, 111403. https://doi.org/10.1016/j.rse.2019.111403.
Hessburg, P. F., & Agee, J. K. (2005). *Dry forests and wildland fires of the inland Northwest USA: Contrasting the landscape ecology of the pre-settlement and modem eras*.
Hilker, T., Wulder, M.A., Coops, N.C., Linke, J., McDermid, G., Masek, J.G., Gao, F., White, J.C., 2009. A new data fusion model for high spatial- and temporal-resolution mapping of forest disturbance based on Landsat and MODIS. *Remote Sens. Environ.* 113 (8), 1613–1627. https://doi.org/10.1016/j.rse.2009.03.007.
Hu, T., Myers Toman, E., Chen, G., Shao, G., Zhou, Y., Li, Y., Zhao, K., Feng, Y., 2021. Mapping fine-scale human disturbances in a working landscape with Landsat time series on Google Earth Engine. *ISPRS J. Photogramm. Remote Sens.* 176, 250–261. https://doi.org/10.1016/j.isprsjprs.2021.04.008.
Hyyppä, E., Kukko, A., Kaijaluoto, R., White, J.C., Wulder, M.A., Pyörälä, J., Liang, X., Yu, X., Wang, Y., Kaartinen, H., Virtanen, J.-P., Hyyppä, J., 2020. Accurate derivation of stem curve and volume using backpack mobile laser scanning. *ISPRS J. Photogramm. Remote Sens.* 161, 246–262. https://doi.org/10.1016/j.isprsjprs.2020.01.018.
Jarron, L., Hermosilla, T., Coops, N., Wulder, M., White, J., Hobart, G., Leckie, D., 2017. Differentiation of alternate harvesting practices using annual time series of landsat data. *Forests* 8 (1), 15. https://doi.org/10.3390/f8010015.
Kangas, A., Maltamo, M., 2006. *Forest inventory: methodology and applications*. Springer.
Kempeneers, P., Soille, P., 2017. Optimizing Sentinel-2 image selection in a Big Data context. *Big Earth Data* 1 (1–2), 145–158. https://doi.org/10.1080/20964471.2017.1407489.
Kennedy, R.E., Yang, Z., Cohen, W.B., 2010. Detecting trends in forest disturbance and recovery using yearly Landsat time series: 1. LandTrendr — Temporal segmentation algorithms. *Remote Sens. Environ.* 114 (12), 2897–2910. https://doi.org/10.1016/j.rse.2010.07.008.
Keselman, H.J., Rogan, J.C., 1977. The Tukey multiple comparison test: 1953–1976. Psychol. Bull. 84 (5), 1050–1056. https://doi.org/10.1037/0033-2909.84.5.1050.
LeDell, E., Petersen, M., Van Der Laan, M., 2015. Computationally efficient confidence intervals for cross-validated area under the ROC curve estimates. *Electronic Journal of Statistics* 9 (1). https://doi.org/10.1214/15-EJS1035.
Li, J., Li, Z.-L., Wu, H., You, N., 2022. Trend, seasonality, and abrupt change detection method for land surface temperature time-series analysis: Evaluation and improvement. *Remote Sens. Environ.* 280, 113222. https://doi.org/10.1016/j.rse.2022.113222.
Meddens, A.J.H., Hicke, J.A., Vierling, L.A., Hudak, A.T., 2013. Evaluating methods to detect bark beetle-caused tree mortality using single-date and multi-date Landsat imagery. *Remote Sens. Environ.* 132, 49–58. https://doi.org/10.1016/j.rse.2013.01.002.
Meigs, G.W., Dunn, C.J., Parks, S.A., Krawchuk, M.A., 2020. Influence of topography and fuels on fire refugia probability under varying fire weather conditions in forests of the Pacific Northwest, USA. Can. J. For. Res. 50 (7), 636–647. https://doi.org/10.1139/cjfr-2019-0406.
Melaas, E.K., Friedl, M.A., Zhu, Z., 2013. Detecting interannual variation in deciduous broadleaf forest phenology using Landsat TM/ETM+ data. *Remote Sens. Environ.* 132, 176–185. https://doi.org/10.1016/j.rse.2013.01.011.
Miller, J.D., Knapp, E.E., Key, C.H., Skinner, C.N., Isbell, C.J., Creasy, R.M., Sherlock, J. W., 2009. Calibration and validation of the relative differenced Normalized Burn Ratio (RdNBR) to three measures of fire severity in the Sierra Nevada and Klamath Mountains, California, USA. *Remote Sens. Environ.* 113 (3), 645–656. https://doi.org/10.1016/j.rse.2008.11.009.
Morin-Bernard, A., Achim, A., Coops, N.C., 2023. Attributing a causal agent and assessing the severity of non-stand replacing disturbances in a northern hardwood

forest using landsat-derived vegetation indices. *Can. J. Remote. Sens.* 49 (1), 2196356. https://doi.org/10.1080/07038992.2023.2196356.
Mulverhill, C., Coops, N.C., Achim, A., 2023. Continuous monitoring and sub-annual change detection in high-latitude forests using Harmonized Landsat Sentinel-2 data. *ISPRS J. Photogramm. Remote Sens.* 197, 309–319. https://doi.org/10.1016/j.isprsjprs.2023.02.002.
NASA. HLS Data Resources. GitHub repository. https://github.com/nasa/HLS-Data-Resources.
Nguyen, H.T., Jones, S., Soto-Berelov, M., Haywood, A., Hislop, S., 2019. Landsat time-series for estimating forest aboveground biomass and its dynamics across space and time: a review. *Remote Sens. (Basel)* 12 (1), 98. https://doi.org/10.3390/rs12010098.
Oliver, C. D., & Larson, B. C. (1996). Forest stand dynamics: Updated edition (Update Edi. ed.). John Wiley & Sons, Inc.
Parks, S.A., Holsinger, L.M., Panunto, M.H., Jolly, W.M., Dobrowski, S.Z., Dillon, G.K., 2018. High-severity fire: Evaluating its key drivers and mapping its probability across Western US forests. *environmental Research Letters 13* (4), 044037. https://doi.org/10.1088/1748-9326/aab791.
Pasquarella, V., Bradley, B., Woodcock, C., 2017. Near-real-time monitoring of insect defoliation using Landsat time series. Forests 8 (8), 275. https://doi.org/10.3390/f8080275.
Pasquarella, V.J., Mickley, J.G., Barker Plotkin, A., MacLean, R.G., Anderson, R.M., Brown, L.M., Wagner, D.L., Singer, M.S., Bagchi, R., 2021. Predicting defoliator abundance and defoliation measurements using Landsat-based condition scores. Remote Sens. Ecol. Conserv. 7 (4), 592–609. https://doi.org/10.1002/rse2.211.
Payette, S., Filion, L., Delwaide, A., 1990. Disturbance regime of a cold temperate forest as deduced from tree-ring patterns: The Tantarè Ecological Reserve, Quebec. Can. J. For. Res. 20 (8), 1228–1241. https://doi.org/10.1139/x90-162.
Peng, C.H., Ma, Z., Lei, X., Zhu, Q., Chen, H., Wang, W., Liu, S., Li, W., Fang, X., Zhou, X., 2011. A drought-induced pervasive increase in tree mortality across Canada's boreal forests. *nature Climate Change 1* (9), 467–471. https://doi.org/10.1038/nclimate1293.
Perez, L., Dragicevic, S., 2009. Modeling mountain pine beetle infestation with an agent-based approach at two spatial scales. Environ. Model. Softw. 25 (2), 223–236. https://doi.org/10.1016/j.envsoft.2009.08.004.
R Core Team. (2021). *R: A language and environment for statistical computing* (Version 4.1.2). R Foundation for Statistical Computing.
Reiche, J., Hamunyela, E., Verbesselt, J., Hoekman, D., Herold, M., 2018. Improving near-real time deforestation monitoring in tropical dry forests by combining dense Sentinel-1 time series with Landsat and ALOS-2 PALSAR-2. *Remote Sens. Environ.* 204, 147–161. https://doi.org/10.1016/j.rse.2017.10.034.
Robin, X., Turck, N., Hainard, A., Tiberti, N., Lisacek, F., Sanchez, J.-C., Müller, M., 2011. pROC: An open-source package for R and S+ to analyze and compare ROC curves. BMC Bioinf. 12 (1), 77. https://doi.org/10.1186/1471-2105-12-77.
Safranyik, L., Carroll, A.L., Régnière, J., Langor, D.W., Riel, W.G., Shore, T.L., Peter, B., Cooke, B.J., Nealis, V.G., Taylor, S.W., 2010. Potential for range expansion of mountain pine beetle into the boreal forest of North America. *Can. Entomol.* 142 (5), 415–442. https://doi.org/10.4039/n08-CPA01.
Senf, C., Pflugmacher, D., Wulder, M.A., Hostert, P., 2015. Characterizing spectral–temporal patterns of defoliator and bark beetle disturbances using Landsat time series. *Remote Sens. Environ.* 170, 166–177. https://doi.org/10.1016/j.rse.2015.09.019.
Seyednasrollah, B., Bowling, D.R., Cheng, R., Logan, B.A., Magney, T.S., Frankenberg, C., Yang, J.C., Young, A.M., Hufkens, K., Arain, M.A., Black, T.A., Blanken, P.D., Bracho, R., Jassal, R., Hollinger, D.Y., Law, B.E., Nesic, Z., Richardson, A.D., 2021. Seasonal variation in the canopy color of temperate evergreen conifer forests. *New Phytol.* 229 (5), 2586–2600. https://doi.org/10.1111/nph.17046.
Shang, R., Zhu, Z., Zhang, J., Qiu, S., Yang, Z., Li, T., Yang, X., 2022. Near-real-time monitoring of land disturbance with harmonized Landsats 7–8 and Sentinel-2 data. *Remote Sens. Environ.* 278, 113073. https://doi.org/10.1016/j.rse.2022.113073.
Shi, H., Tian, H., Lange, S., Yang, J., Pan, S., Fu, B., Reyer, C.P.O., 2021. Terrestrial biodiversity threatened by increasing global aridity velocity under high-level warming. *Proc. Natl. Acad. Sci.* 118 (36), e2015552118. https://doi.org/10.1073/pnas.2015552118.
Smith-Tripp, S.M., Coops, N.C., Mulverhill, C., White, J.C., Axelson, J., 2024. Landsat assessment of variable spectral recovery linked to post-fire forest structure in dry sub-boreal forests. ISPRS J. Photogramm. Remote Sens. 208, 121–135. https://doi.org/10.1016/j.isprsjprs.2024.01.008.
Stone, C., Chisholm, L., Coops, N., 2001. Spectral reflectance characteristics of eucalypt foliage damaged by insects. Aust. J. Bot. 49 (6), 687. https://doi.org/10.1071/BT00091.
Swanson, M.E., Franklin, J.F., Beschta, R.L., Crisafulli, C.M., DellaSala, D.A., Hutto, R.L., Lindenmayer, D.B., Swanson, F.J., 2011. The forgotten stage of forest succession: Early-successional ecosystems on forest sites. *Front. Ecol. Environ.* 9 (2), 117–125. https://doi.org/10.1890/090157.
Thompson, I.D., Maher, S.C., Rouillard, D.P., Fryxell, J.M., Baker, J.A., 2007. Accuracy of forest inventory mapping: Some implications for boreal forest management. *For. Ecol. Manage.* 252 (1–3), 208–221. https://doi.org/10.1016/j.foreco.2007.06.033.
Tompalski, P., Coops, N.C., White, J.C., Goodbody, T.R.H., Hennigar, C.R., Wulder, M.A., Socha, J., Woods, M.E., 2021. Estimating changes in forest attributes and enhancing growth projections: A review of existing approaches and future directions using airborne 3D point cloud data. *current Forestry Reports 7* (1), 1–24. https://doi.org/10.1007/s40725-021-00135-w.
Van Mantgem, P.J., Stephenson, N.L., Byrne, J.C., Daniels, L.D., Franklin, J.F., Fulé, P.Z., Harmon, M.E., Larson, A.J., Smith, J.M., Taylor, A.H., Veblen, T.T., 2009. Widespread increase of tree mortality rates in the Western United States. *Science* 323 (5913), 521–524. https://doi.org/10.1126/science.1165000.
Varhola, A., Coops, N.C., Bater, C.W., Teti, P., Boon, S., Weiler, M., 2010. The influence of ground- and lidar-derived forest structure metrics on snow accumulation and ablation in disturbed forests. Can. J. For. Res. 40 (4), 812–821. https://doi.org/10.1139/x10-008.
Verbesselt, J., Hyndman, R., Newnham, G., Culvenor, D., 2010. Detecting trend and seasonal changes in satellite image time series. *Remote Sens. Environ.* 114 (1), 106–115. https://doi.org/10.1016/j.rse.2009.08.014.
Westfall, J., Ebata, T., HR GISolutions, I. (2019). Forest Health Aerial Overview Survey Standards for British Columbia.
White, J.C., Wulder, M.A., Hobart, G.W., Luther, J.E., Hermosilla, T., Griffiths, P., Coops, N.C., Hall, R.J., Hostert, P., Dyk, A., Guindon, L., 2014. Pixel-based image compositing for large-area dense time series applications and science. *Can. J. Remote. Sens.* 40 (3), 192–212. https://doi.org/10.1080/07038992.2014.945827.
White, J.C., Coops, N.C., Wulder, M.A., Vastaranta, M., Hilker, T., Tompalski, P., 2016. Remote sensing technologies for enhancing forest inventories: A review. *Canadian Journal of Remote Sensing 42* (5), 619–641. https://doi.org/10.1080/07038992.2016.1207484.
White, J.C., Wulder, M.A., Hermosilla, T., Coops, N.C., Hobart, G.W., 2017. A nationwide annual characterization of 25 years of forest disturbance and recovery for Canada using Landsat time series. *remote Sensing of Environment 194*, 303–321. https://doi.org/10.1016/j.rse.2017.03.035.
Woodcock, C.E., Allen, R., Anderson, M., Belward, A., Bindschadler, R., Cohen, W., Gao, F., Goward, S.N., Helder, D., Helmer, E., Nemani, R., Oreopoulos, L., Schott, J., Thenkabail, P.S., Vermote, E.F., Vogelmann, J., Wulder, M.A., Wynne, R., 2008. Free access to Landsat imagery. *science 302* (5879), 1011. https://doi.org/10.1126/science.320.5879.1011a.
Woods, K.D., Kern, C.C., 2022. Intermediate disturbances drive long-term fluctuation in old-growth forest biomass: An 84-yr temperate forest record. *Ecosphere* 13 (1). https://doi.org/10.1002/ecs2.3871.
Woods, K. D. (2000). *Dynamics in Late-Successional Hemlock-Hardwood Forests over Three Decades*.
Wulder, M.A., Coops, N.C., 2014. Satellites: Make Earth observations open access. *Nature 513*, 30–31. https://doi.org/10.1038/513030a.
Wulder, M.A., White, J.C., Bentz, B.J., Ebata, T., 2006. Augmenting the existing survey hierarchy for mountain pine beetle red-attack damage with satellite remotely sensed data. *For. Chron.* 82 (2), 187–202. https://doi.org/10.5558/tfc82187-2.
Wulder, M.A., White, J.C., Cranny, M.M., Hall, R.J., Luther, J.E., Beaudoin, A., Dechka, J. A., 2008. Monitoring Canada' s forests. Part 1: Completion of the EOSD land cover project. Can. J. Remote. Sens. Vol. 34 (6), 549–562. https://doi.org/10.5589/m08-066.
Wulder, M.A., Roy, D.P., Radeloff, V.C., Loveland, T.R., Anderson, M.C., Johnson, D.M., Healey, S., Zhu, Z., Scambos, T.A., Pahlevan, N., Hansen, M., Gorelick, N., Crawford, C.J., Masek, J.G., Hermosilla, T., White, J.C., Belward, A.S., Schaaf, C., Woodcock, C.E., Cook, B.D., 2022. Fifty years of Landsat science and impacts. *Remote Sens. Environ.* 280, 113195. https://doi.org/10.1016/j.rse.2022.113195.
Yang, L., Jin, S., Danielson, P., Homer, C., Gass, L., Bender, S.M., Case, A., Costello, C., Dewitz, J., Fry, J., Funk, M., Granneman, B., Liknes, G.C., Rigge, M., Xian, G., 2018. A new generation of the United States National Land Cover Database: Requirements, research priorities, design, and implementation strategies. *ISPRS J. Photogramm. Remote Sens.* 146, 108–123. https://doi.org/10.1016/j.isprsjprs.2018.09.006.
Ye, S., Rogan, J., Zhu, Z., Hawbaker, T.J., Hart, S.J., Andrus, R.A., Meddens, A.J.H., Hicke, J.A., Eastman, J.R., Kulakowski, D., 2021. Detecting subtle change from dense Landsat time series: Case studies of mountain pine beetle and spruce beetle disturbance. *Remote Sens. Environ.* 263, 112560. https://doi.org/10.1016/j.rse.2021.112560.
Zald, H.S., Dunn, C.J., 2018. Severe fire weather and intensive forest management increase fire severity in a multi-ownership landscape. *Ecological Applications 28* (4), 1068–1080. https://doi.org/10.1002/eap.1710.
Zhao, K., Wulder, M.A., Hu, T., Bright, R., Wu, Q., Qin, H., Li, Y., Toman, E., Mallick, B., Zhang, X., Brown, M., 2019. Detecting change-point, trend, and seasonality in satellite time series data to track abrupt changes and nonlinear dynamics: A Bayesian ensemble algorithm. *Remote Sens. Environ.* 232, 111181. https://doi.org/10.1016/j.rse.2019.04.034.
Zhu, Z., Woodcock, C.E., 2014. Continuous change detection and classification of land cover using all available Landsat data. *Remote Sens. Environ.* 144, 152–171. https://doi.org/10.1016/j.rse.2014.01.011.